

# CrystEngComm

Accepted Manuscript



This is an *Accepted Manuscript*, which has been through the Royal Society of Chemistry peer review process and has been accepted for publication.

*Accepted Manuscripts* are published online shortly after acceptance, before technical editing, formatting and proof reading. Using this free service, authors can make their results available to the community, in citable form, before we publish the edited article. We will replace this *Accepted Manuscript* with the edited and formatted *Advance Article* as soon as it is available.

You can find more information about *Accepted Manuscripts* in the [Information for Authors](#).

Please note that technical editing may introduce minor changes to the text and/or graphics, which may alter content. The journal's standard [Terms & Conditions](#) and the [Ethical guidelines](#) still apply. In no event shall the Royal Society of Chemistry be held responsible for any errors or omissions in this *Accepted Manuscript* or any consequences arising from the use of any information it contains.

# Synergetic functional properties in two-component single amino acid-based hydrogels

Galit Fichman,<sup>a</sup> Tom Guterman,<sup>a</sup> Lihi Adler-Abramovich<sup>a</sup> and Ehud Gazit<sup>\*ab</sup>

a. Department of Molecular Microbiology and Biotechnology, George S. Wise Faculty of Life Sciences, Tel Aviv University, Tel Aviv 6997801, Israel.

b. Department of Materials Science and Engineering, Iby and Aladar Fleischman Faculty of Engineering, Tel Aviv University, Tel Aviv 6997801, Israel.

\*To whom correspondence should be addressed at ehudg@post.tau.ac.il

## Abstract

The formation of hydrogels by low molecular weight building blocks results in important supramolecular assemblies for technological applications. *N*-modified amino acids are especially interesting components for the organization of such structures due to the high efficiency of association, inherent biocompatibility, and structural diversity. The fluorenylmethoxycarbonyl (Fmoc)-modified tyrosine (Fmoc-Tyr) has been extensively studied as a notably simple yet highly efficient hydrogelator. Here we present the ability to use a combination of Fmoc-Tyr and the catechol-containing Fmoc-3,4-dihydroxyphenylalanine (Fmoc-DOPA) to form a functional

two-component hydrogel which combines the physical characteristics as observed with Fmoc-Tyr hydrogels together with the functionality of the catechol groups. We demonstrate that a combination of the two building blocks results in the rapid formation of three-dimensional self-supporting gels. Rheological analysis indicated that the observed hybrid gel has very high storage modulus, in the same order of magnitude as that of the Fmoc-Tyr gel. In addition to the envisioned mechanical properties, the combined gel also displayed a clear silver ion reduction activity. Taken together, we illustrate the ability to utilize two-component gels to achieve synergetic properties, combining rigidity and functionality.

## Introduction

The formation of supramolecular assemblies from peptide building blocks has drawn significant attention over the last decade due to the attractive functional and diverse properties exhibited by these systems, including responsiveness to stimuli, unique physicochemical traits and the facile decoration by desired functional groups using various biological and chemical methods.<sup>1-5</sup> Different classes of supramolecular peptide assemblies possess the ability to form visco-elastic hydrogels with underlying nano-scale order.<sup>6-9</sup> In these systems, the self-assembled fibrillar structures are formed *via* non-covalent interactions between low molecular weight (LMW) peptide building blocks. These fibrillar structures entangle and interact, thus leading to immobilization of water molecules in a gel phase that results in a distinctive three-dimensional macroscopic structure. Supramolecular hydrogels formed by different building blocks vary in their physical properties. The mechanical properties could also be affected by the gelation triggering method.<sup>10-12</sup> These methods include enzymatic triggering,<sup>13</sup> temperature-dependent gelation<sup>14</sup> or gelation following a change in the molecular environment of the hydrogelator, such as modulation of the ionic strength,<sup>15</sup> the pH,<sup>16, 17</sup> or the identity of the solvent.<sup>18</sup> The diverse

rheological characteristics and gel functionalities represent attractive properties for drug delivery,<sup>19</sup> tissue engineering,<sup>20</sup> and other potential technological applications.<sup>21</sup>

A subset of peptide building blocks which possess a distinct propensity to form supramolecular hydrogels comprises the very short aromatic *N*-fluorenylmethoxycarbonyl (Fmoc)-modified peptides and the related Fmoc-modified aromatic single amino acids (FASAA). This class of hydrogelators holds key advantages which include simple and cost-effective synthesis, efficient gelation at low concentrations (around 0.1-2 % wt) and rapid gelation kinetics, with the resulting hydrogels being potentially biocompatible,<sup>22, 23</sup> biodegradable and endowed with anti-inflammatory properties.<sup>24, 25</sup> Fmoc-modified aromatic peptides and amino acids are simple amphiphilic molecules whose self-assembly is driven by a combination of  $\pi$ - $\pi$  interactions between planar aromatic moieties and hydrogen bonding, leading to the formation of  $\beta$ -sheet-like ordered structures.<sup>26</sup> FASAAs are the minimal representation of this class of hydrogelators and studies of these compounds have focused on FASAA analogues of coded amino acids, namely Fmoc-phenylalanine (Fmoc-Phe) and Fmoc-tyrosine (Fmoc-Tyr). Fmoc-Tyr was the first investigated FASAA and was shown to form hydrogel following the enzymatic dephosphorylation of Fmoc-Tyr phosphate.<sup>13</sup> Later studies reported the pH-dependent gelation of Fmoc-Tyr, where a gradual decrease in pH from alkaline to acidic led to protonation of the carboxylate group and to the subsequent conversion of solubilized Fmoc-Tyr to ordered fibrillar assemblies in a gel matrix.<sup>17, 27-29</sup> Additionally, solvent-switch gelation triggering of Fmoc-Tyr was reported, where Fmoc-Tyr was initially solubilized in dimethyl sulfoxide (DMSO) followed by dilution into water.<sup>30</sup> FASAAs derivatives of non-coded amino acids have also been investigated as hydrogelators. Several examples include the fluorinated Fmoc-Phe derivatives,<sup>30</sup> naphthyl-modified Fmoc-alanine<sup>31</sup> and Fmoc-3,4-dihydroxyphenylalanine (Fmoc-DOPA).<sup>32, 33</sup>

Fmoc-DOPA is especially interesting due to the multifunctional nature of the catecholic moiety, which is capable to act as an antioxidant, radical trapper, metal chelator, oxidizable reducing agent, etc.<sup>34, 35</sup> Self-assembling DOPA-containing short peptides have been reported<sup>36-38</sup> and Fmoc-DOPA was recently shown to act as a minimal DOPA-containing gelator which forms mechanically weak hydrogels.<sup>32</sup>

In this work, we examined the self-assembly and combined hydrogelation of the structurally-related Fmoc-Tyr and Fmoc-DOPA (Fig. 1). Multicomponent supramolecular gels, composed of more than one LMW component that can undergo self-assembly and gelation, have been relatively unexplored and are the subject of current research in this field.<sup>39</sup> It has been demonstrated that hybrid supramolecular gels can possess improved or synergistic traits with regard to the mechanical strength of the gel,<sup>40-43</sup> the gelation efficiency<sup>44</sup> and the functionality of the resulting material.<sup>45, 46</sup> Fmoc-modified short peptides, as well as single amino acids, were used for the formation of two-component hydrogels, with the second component being an Fmoc-modified or unmodified short peptide or amino acid.<sup>13, 31, 47-50</sup> Here, we demonstrate the ability to obtain hybrid gels which combine chemical properties of one building block and physical properties of the other. Specifically, we designed rigid redox-active hydrogels based on the well-known Fmoc-Tyr hydrogelator and the recently introduced Fmoc-DOPA hydrogelator. The characterization of the two-component hydrogels was performed using electron microscopy, vibrational and fluorescence spectroscopy and rheological assays. Furthermore, we examined the ability of the hydrogels to reduce ionic silver using UV-Vis spectroscopy and electron microscopy. The hybrid hydrogels mechanically resembled the Fmoc-Tyr hydrogels, which are superior to those of Fmoc-DOPA from the rheological aspect, while bearing the functionality presented by the catecholic group of Fmoc-DOPA.

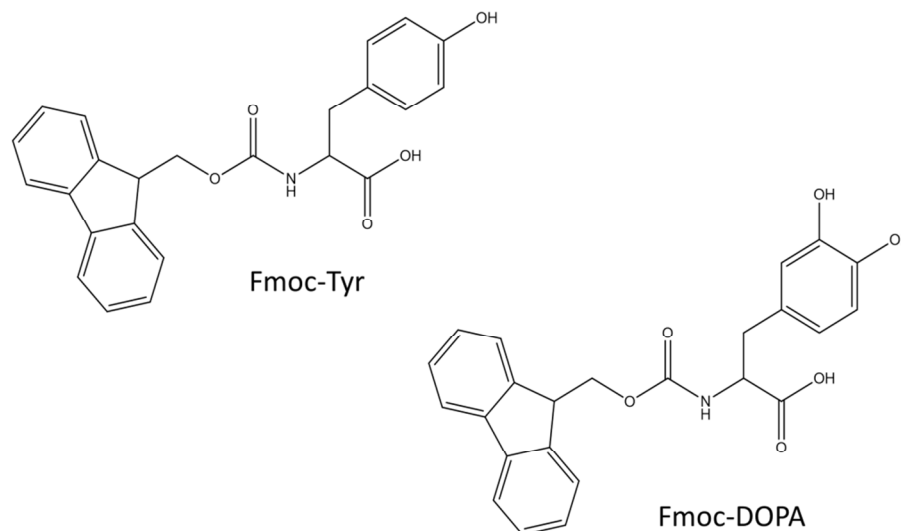


**Fig. 1** Chemical structures of *N*-fluorenylmethoxycarbonyl-tyrosine (Fmoc-Tyr) and *N*-fluorenylmethoxycarbonyl-3,4-dihydroxyphenylalanine (Fmoc-DOPA) low molecular weight (LMW) hydrogelators.

## Experimental

### Preparation of Assemblies

The Fmoc-Tyr and Fmoc-DOPA modified amino acids were purchased from Sigma-Aldrich and AnaSpec, respectively. The FASAA building blocks were purified to 97–98%. For the formation of Fmoc-Tyr and Fmoc-DOPA assemblies, lyophilized FASAA were dissolved in DMSO to a concentration of 100 mg/mL then diluted with Milli-Q water to the desired final concentration (1.25, 1.67, 3.5 or 5 mg/mL). For the formation of hybrid assemblies, lyophilized building blocks were separately dissolved in DMSO to a concentration of 100 mg/mL then mixed accordingly to the desired Fmoc-Tyr:Fmoc-DOPA ratio (1:1 when the final concentration of the mixed building

blocks was 10 mg/mL, and 3:1 when the final concentration of the mixed building blocks was either 5 or approximately 6.7 mg/mL).

### **Transmission electron microscopy (TEM)**

TEM analysis was performed by applying 10  $\mu\text{L}$  samples to 400-mesh copper grids covered by carbon-stabilized Formvar film (SPI, West Chester, PA). The samples were allowed to adsorb for 2 min before excess fluid was blotted off. For samples that were negatively stained, 10  $\mu\text{L}$  of 2% uranyl acetate was then deposited on the grid and allowed to adsorb for 2 min before excess fluid was blotted off. TEM micrographs were recorded using Tecnai-12 electron microscope (Tokyo, Japan) operating at 120 kV.

### **Rheology**

Rheological measurements for *in situ*-formed hydrogels were performed using an ARES-G2 rheometer (TA Instruments, New Castle, DE, USA). Time-sweep oscillatory tests in 20 mm parallel plate geometry were conducted at 0.7% strain and 10 rad/sec frequency on 200  $\mu\text{L}$  of fresh solutions (resulting in a gap size of about 0.6 mm), 1 min after their preparation. In order to determine the linear viscoelastic region, oscillatory strain (0.01–100%) and frequency sweep (0.01–100 Hz) tests were conducted 40 min after diluting the DMSO stock solution into Milli-Q water. All rheology tests were done in triplicates and averaged. To investigate the mechanical properties of silver-containing hydrogels, rheological measurements were performed on hybrid gels that were pre-prepared in the presence or absence of silver nitrate. Stock solution of the desired Fmoc-Tyr:Fmoc-DOPA ratio was diluted into either silver nitrate aqueous solutions or into water and immediately deposited into Press-To-Seal silicone isolators (Sigma Aldrich, Israel) adhered to glass surfaces. Prior to measurements, all gels were incubated for 2 days at

room temperature in the presence of ambient light. Incubation was performed in sealed humid containers to avoid dehydration. Rheological measurements were made using 8 mm parallel plate geometry where frequency-sweep measurements were performed under a strain of 0.2% and strain amplitude measurements were conducted at a frequency of 1 Hz.

### **Turbidity Analysis**

Turbidity analysis for Fmoc-Tyr, Fmoc-DOPA and Fmoc-Tyr:Fmoc-DOPA hybrids preparations was conducted for freshly prepared solutions. 240  $\mu\text{L}$  aliquots were pipetted into a 96-well plate and absorbance at 405 nm was measured for 2 h, starting 1 min after the preparation of the solutions. All measurements were performed using a Biotek Synergy HT plate reader (Winooski, VT, USA) at 25  $^{\circ}\text{C}$ .

### **Fourier-transform infrared (FTIR) spectroscopy**

FTIR spectroscopy was performed with a portion of pre-prepared samples of gels, prepared as described above, 3 days after the initiation of assembly. The samples (5 mg/mL Fmoc-Tyr gel, 1.67 mg/mL Fmoc-DOPA gel and 3:1 Fmoc-Tyr:Fmoc-DOPA hybrid gel at 6.67 mg/mL) were deposited onto disposable KBr IR sample cards (Sigma-Aldrich, Israel), which were then allowed to dry under vacuum. Transmission infrared spectra were collected using Nexus 470 FTIR spectrometer (Nicolet, Offenbach, Germany) with a deuterated triglycine sulfate (DTGS) detector. Measurements were performed using the atmospheric suppression mode, by averaging 64 scans in 4  $\text{cm}^{-1}$  resolution.

### **Fluorescence spectroscopy**

The emission spectra of gels at concentrations of 3.5 or 5 mg/mL for Fmoc-Tyr, 1.25 or 1.67 mg/mL for Fmoc-DOPA and 3:1 Fmoc-Tyr:Fmoc-DOPA for at 5 or 6.67 mg/mL for the hybrid

gels were recorded 3 days after the initiation of assembly using a Horiba Jobin Yvon FL3-11 fluorimeter (Horiba Jobin Yvon, NJ, USA). A quartz cuvette with an optical path length of 1 cm was used. The experiments were carried out using an excitation wavelength of 280 nm and 5 nm excitation and emission slits.

### **Ionic silver reduction**

Silver reduction assay was performed with gels prepared from the individual Fmoc-Tyr and Fmoc-DOPA gelators and their 3:1 hybrid. To examine silver reduction using UV-Vis spectroscopy, samples were prepared as described above when 200  $\mu\text{L}$  aliquots of solution were pipetted into 96-well UV-Star UV transparent plates (Greiner BioOne, Frickenhausen, Germany). After 1 day of incubation at room temperature, 40  $\mu\text{L}$  of either 2 mM silver nitrate solution or Milli-Q water were pipetted into the pre-prepared gel samples, resulting with 5 mg/mL Fmoc-Tyr, 1.67 mg/mL Fmoc-DOPA and 3:1 hybrid at 6.67 mg/mL gel including or excluding 0.33 mM silver nitrate. The samples were then incubated at room temperature either exposed to or sheltered from light and their UV-Vis spectra were collected after 5 days using a Biotek Synergy HT plate reader over the range of 350-550 nm. To monitor the kinetics of ionic silver reduction, the assay was performed as described above when following the addition of 40  $\mu\text{L}$  silver nitrate or water, absorbance at 445 nm was monitored over five days for gels pre-prepared from either 1.67 mg/mL Fmoc-DOPA gelator or Fmoc-Tyr:Fmoc-DOPA 3:1 gelators at 6.67 mg/mL. The gels were incubated while exposed to ambient light. Each data point represents the subtraction result of samples incubated without silver nitrate from the silver nitrate-added samples and is an average of four repeats. The time-dependent increase in absorbance at 445 nm over five days, for both the Fmoc-DOPA and hybrid gels, fitted the Boltzmann equation:

$$\Delta A(t) = \frac{\Delta A_i - \Delta A_f}{1 + e^{-\frac{t-t_{50}}{dt}}} + \Delta A_f \quad (1)$$

where  $\Delta A(t)$  is the absorbance at 445 nm at incubation time  $t$ ,  $\Delta A_i$  is the  $\Delta A$  at the initial data point,  $\Delta A_f$  is the  $\Delta A$  at infinite time and  $t_{50}$  is the time at which the  $\Delta A$  is equal to one-half the  $\Delta A_f$ . During the first 8 hours, the time-dependent increase in absorbance at 445 nm for Fmoc-DOPA fitted the Boltzmann equation, whereas the time-dependent increase in absorbance at 445 nm in the case of the hybrid gels fitted the exponential equation:

$$\Delta A(t) = 0.08799 - 0.08165e^{-0.23007t} \quad (2)$$

where  $\Delta A(t)$  is the absorbance at 445 nm at incubation time  $t$ .

## Results and discussion

The assembly of each FASAA and the subsequent formation of the hybrid gels was induced by employing the solvent-switch method. Specifically, the self-assembly of the individual Fmoc-Tyr and Fmoc-DOPA building blocks was triggered by solvent-switch of a 100 mg/mL DMSO stock solution into water and the gelation of the hybrid gels was initiated similarly, with a DMSO stock solution containing a mixture of the dissolved FASAAs at molar ratios of 1:1 and 3:1 (Fmoc-Tyr:Fmoc-DOPA). A turbidity change accompanied the dilution of Fmoc-Tyr, Fmoc-DOPA and the hybrid stock solutions into water, as all samples instantly became opaque and gradually appeared clearer. In parallel to this turbidity change, the Fmoc-Tyr and hybrid solutions exhibited self-supporting gel characteristics within minutes after triggering of the assembly, as was indicated by simple qualitative vial-inversion observations (Fig. 2a), while the Fmoc-DOPA preparations did not form a self-supporting architecture under these conditions.

Following these observations, we investigated the individual Fmoc-DOPA and Fmoc-Tyr hydrogelators. The Fmoc-DOPA preparations were viscous and presented weak gel-like

behavior, as previously reported.<sup>32</sup> TEM imaging of the weak Fmoc-DOPA gel revealed fibrillar assemblies which appeared linear, unbranched and extending to the length of micrometers (Fig. 2b). The width of the fibers ranged from 5 to 10 nm and lateral bundling was observed. The obtained Fmoc-Tyr hydrogels were semi-transparent and presented similar underlying fibers, albeit wider, with an approximated width of 15 nm, as imaged by TEM (Fig 2b). These observations are in line with previous reports concerning the hydrogelation of Fmoc-Tyr by using the solvent-switch method.<sup>30</sup> Next, we examined the hybrid hydrogels. These gels presented similar macroscopic behavior to those of Fmoc-Tyr and similar fibrillar assemblies of 15 nm in width were imaged by TEM (Fig. 2b).

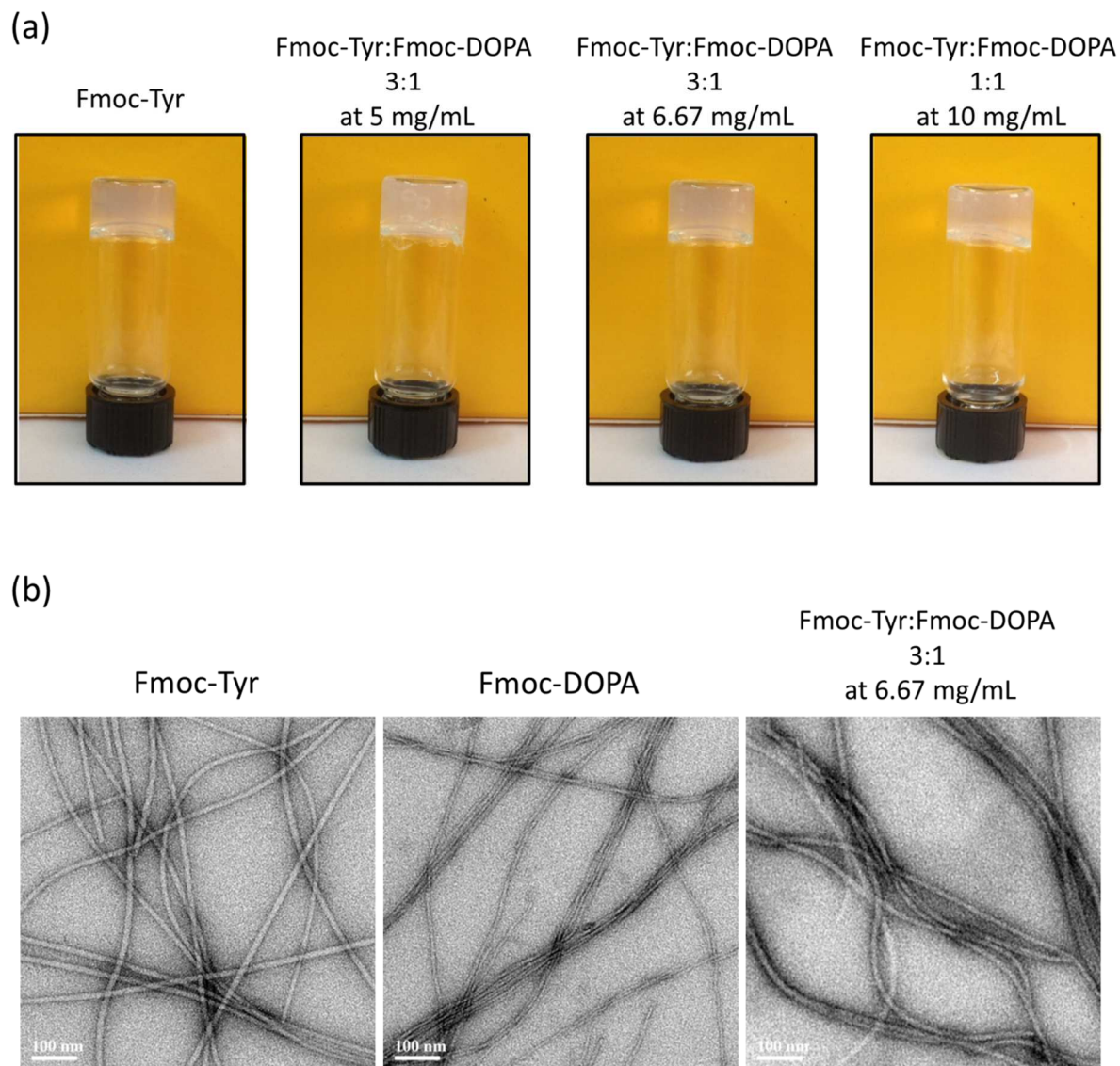


**Fig. 2** Macroscopic observation and imaging of hybrid gels; (a) Photographs of inverted vials containing preparations of 5 mg/mL Fmoc-Tyr and Fmoc-Tyr:Fmoc-DOPA two-component gels at different concentrations. (b) Transmission electron microscopy (TEM) micrographs of an Fmoc-Tyr hydrogel, Fmoc-DOPA preparation, and the two-component hydrogel.

To better understand the organization and assembly kinetics, we monitored the change in turbidity over time of the individual and combined gelators by measuring the absorbance at 405 nm (Fig. 3). While the turbidity of Fmoc-DOPA preparations showed little change during the experimental time frame of 100 minutes, Fmoc-Tyr preparations presented a gradual step-wise

decrease, resulting in a significantly lower turbidity already within less than 10 minutes. Furthermore, the turbidity kinetics and end-point values did not seem to change markedly for the concentrations tested albeit the higher initial value for the higher concentration. Interestingly, the hybrid preparations presented a unique, third behavior with an apparent lag period, a gradual decrease in turbidity and an end-point value in the range between that of the individual hydrogelators (Fig. 3). This behavior was observed for both Fmoc-Tyr:Fmoc-DOPA ratios tested. Similar gradual clearance of hydrogel preparations after an initial opaque stage was observed with other cases of peptide-based LMW hydrogelators. Two alternative models were suggested to explain the mechanism of decrease in absorbance. The first model suggests that this behavior may reflect a slow process of organization following a rapid phase of hydrophobic collapse.<sup>38</sup> According to the second model, it may be the result of a phase separation process where a fibrous network is formed at the expense of unstable spherical assemblies.<sup>51</sup>

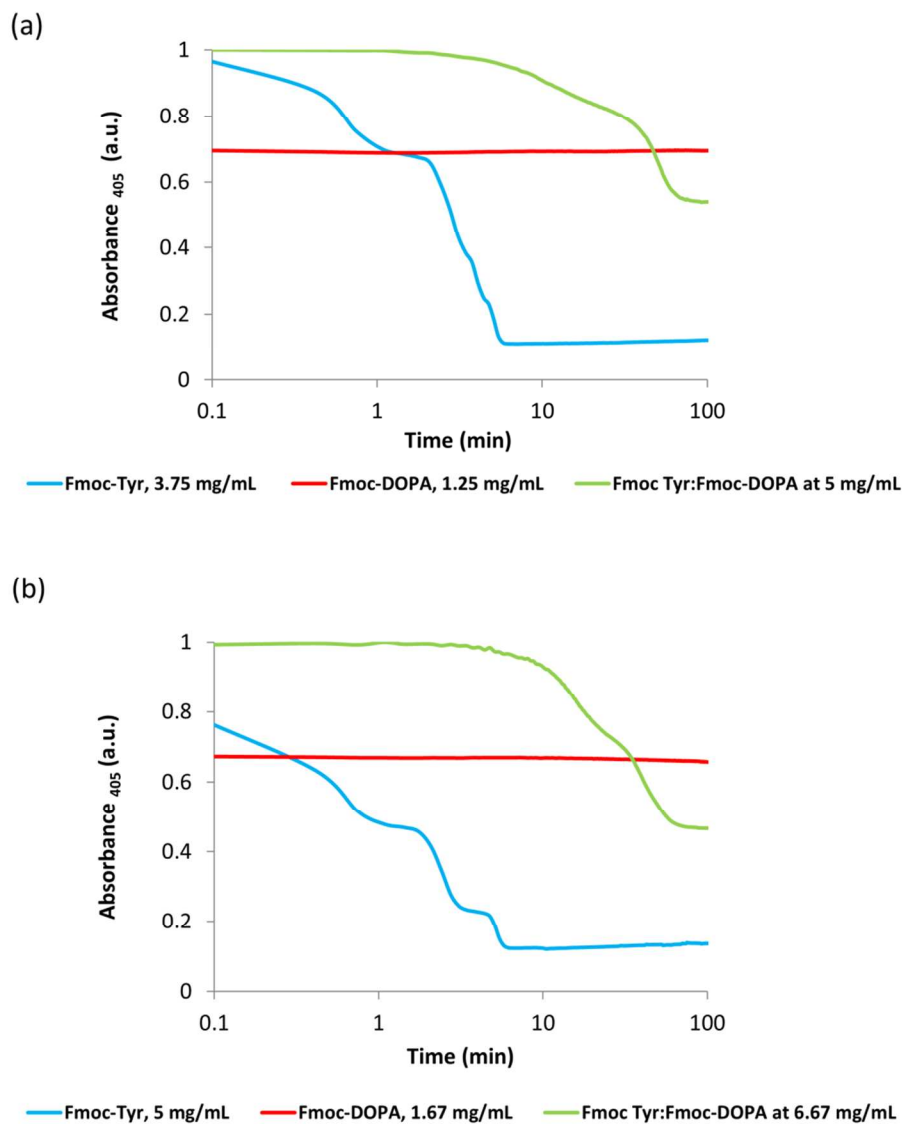


**Fig. 3** Kinetics of absorbance at 405 nm for Fmoc-Tyr gels, Fmoc-DOPA preparations and Fmoc-Tyr:Fmoc-DOPA 3:1 hybrid gels at different concentrations. Absorbance values were normalized. Logarithmic axis is used due to time-scale differences in the optical clearance rate of the different compounds.

Next, we characterized the visco-elastic properties of the Fmoc-Tyr and hybrid hydrogels; preparations of Fmoc-DOPA alone did not present sufficient mechanical rigidity as required for this assay. Time-sweep rheological measurements at the linear regime (Fig. S1) were performed

to monitor the gelation kinetics and to measure the storage modulus of the fully-formed gels at a time frame of 30 min (Fig. 4); this time frame was selected in order to avoid dehydration-related artifacts. For 5 mg/mL Fmoc-Tyr, the gelation was rapid with the final storage modulus of approximately 30 kPa measured after about 20 min. The measured storage modulus is of the highest measured for Fmoc-Tyr hydrogels<sup>11, 30</sup> and this is likely due to the higher concentration of the gelator used in this work. Similar rheological behavior was observed for the 3:1 Fmoc-Tyr:Fmoc-DOPA hybrids, at 5 and 6.67 mg/mL, which presented storage moduli in the same order of magnitude of Fmoc-Tyr and similar gelation kinetics. However, a marked difference in the overall kinetics profile of the hybrids, compared to that of Fmoc-Tyr, was observed. Unlike the prompt gelation of the Fmoc-Tyr, there was a lag phase for both hybrids, especially in the case of the Fmoc-Tyr:Fmoc-DOPA at 5 mg/mL concentration. The lag-phase may reflect an internal organization of the two-component system in which the ratio of the two hydrogelators dictates the rate of assembly and subsequent gelation.

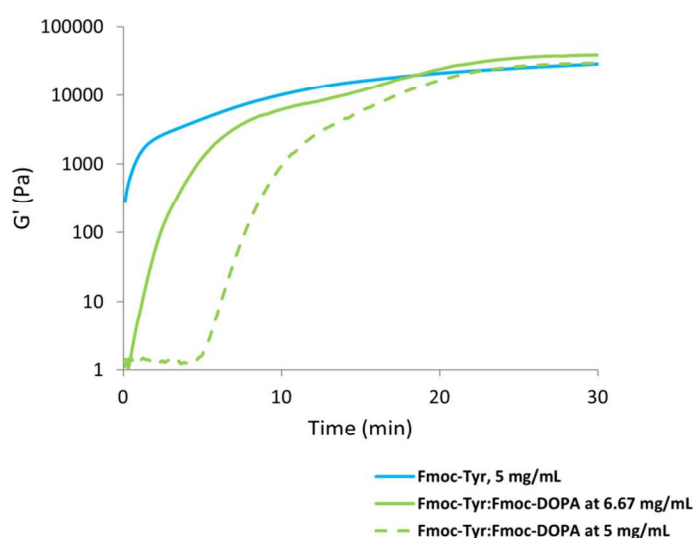


**Fig. 4** Rheological properties of the hydrogels. Gelation kinetics of Fmoc-Tyr and Fmoc-Tyr:Fmoc-DOPA 3:1 hybrid at different concentrations at 25 °C. Measurements were conducted at 0.7% strain and 10 rad/sec frequency.

To compare the internal organization of the hydrogels we employed FTIR spectroscopy (Fig. 5a). For all three gels, peaks were present at 1411 and 1445  $\text{cm}^{-1}$  and may be assigned to tyrosine carboxylate and aromatic ring stretching vibrations, respectively.<sup>52</sup> In the amide II region, the peak position was 1516  $\text{cm}^{-1}$  for Fmoc-Tyr and the hybrid gel, as opposed to 1528  $\text{cm}^{-1}$  for Fmoc-DOPA. In the amide I region, a peak at 1616  $\text{cm}^{-1}$  was present for Fmoc-Tyr and the hybrid gel, while appearing relatively attenuated and shifted to 1610  $\text{cm}^{-1}$  in the Fmoc-DOPA spectrum. The amide I band corresponds to amide C=O stretching and in proteins and peptide the  $\beta$ -sheet conformation is usually linked to the above specific positions,<sup>53</sup> yet in the case of FASAA such interpretation may not be straightforward. Two closely positioned bands were present in all spectra, at approximately 1695 and 1718  $\text{cm}^{-1}$ , ascribed respectively to the Fmoc carbamate group<sup>54</sup> and to hydrogen-bonded tyrosine carboxyl.<sup>55</sup> Finally, a broad band was present in all three spectra above 3000  $\text{cm}^{-1}$ , with the band centered at 3328  $\text{cm}^{-1}$  for Fmoc-Tyr and at 3408  $\text{cm}^{-1}$  for Fmoc-DOPA and the hybrid gel; this region corresponds to stretching vibrations of NH and OH.<sup>52</sup> Interestingly, all features observed for the hybrid hydrogel were also present in either individual gel, with no other, unique features appearing in the spectrum of the hybrid gel. This implies that the combined presence of the individual gelators in the hybrid gel does not significantly alter their molecular organization. To further structurally compare the gels, we used fluorescence spectroscopy. All three hydrogels gave resembling spectra, with an emission peak at 316 nm and no significant broadening of the peak (Fig. 5b). Taken together, these data indicate a general similarity in the internal organization of the hybrid hydrogel and the individual hydrogels.

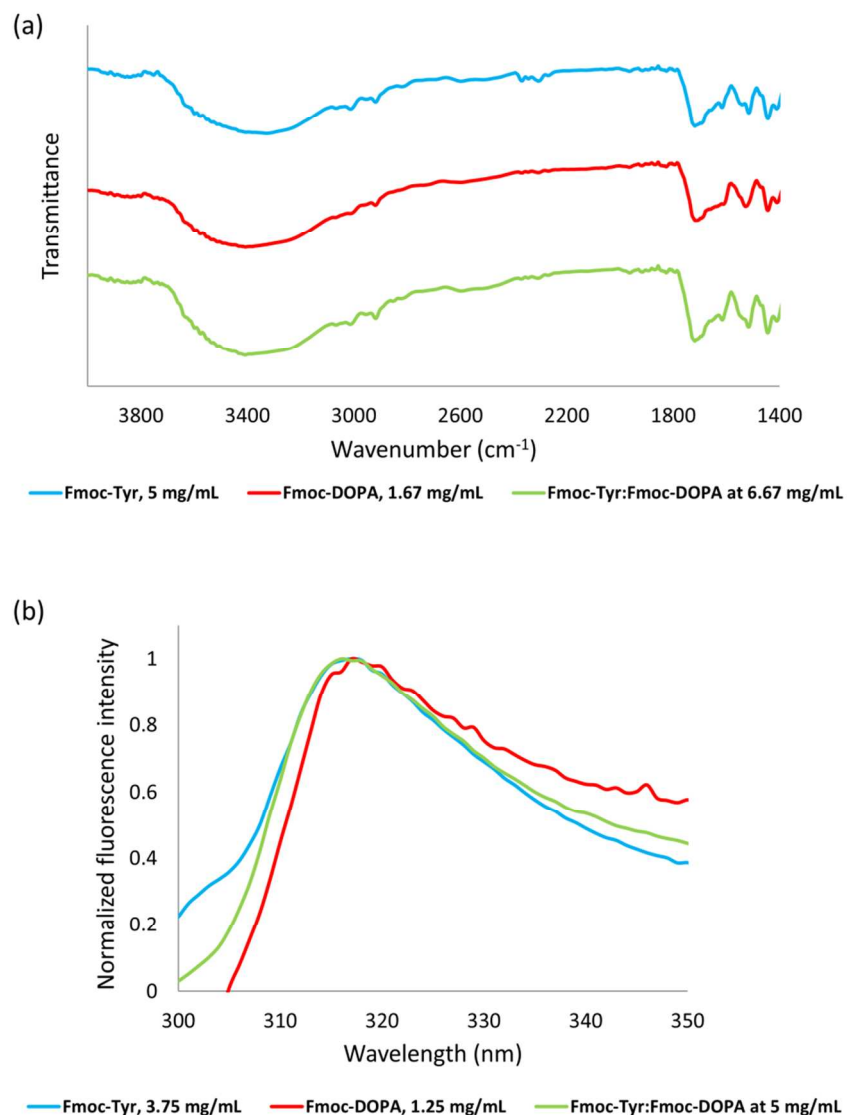


**Fig. 5** Spectroscopic characterization of individual and hybrid gels; (a) Fourier transform infrared (FTIR) and (b) fluorescence emission spectra of gels prepared from the individual Fmoc-Tyr and Fmoc-DOPA gelators and from their 3:1 hybrid at different concentrations. Spectra were taken 3 days after the initiation of assembly. All spectra were normalized. FTIR spectra were vertically offset for clarity.

Finally we studied the functional properties of the hybrid hydrogels and examined their ability to reduce ionic silver. Reduction of silver ions into silver nanoparticles (AgNP) may have various technological applications.<sup>56, 57</sup> There are several inductive and spontaneous methods for the

preparation of AgNP.<sup>57, 58</sup> One simple spontaneous method utilizes the redox-active catechol group of DOPA.<sup>34</sup> Catechol-modified polyethylene glycol (PEG)-based polymers are capable of spontaneous redox activity at alkaline pH that leads to the formation of silver nanoparticles.<sup>59, 60</sup> DOPA-containing supramolecular peptide assemblies were demonstrated to facilitate both spontaneous silver nanoparticles formation<sup>37, 38</sup> and seamless metallic coating of the assemblies,<sup>38</sup> under mildly acidic conditions. In the context of supramolecular peptide assemblies and hydrogels, inductive AgNP and silver nanoclusters preparation by exposure to ambient light has been reported.<sup>61, 62, 63</sup> In these studies, the reduction of ionic silver was ascribed to carboxylate moieties in the peptides which were able to bind silver ions and enable their reduction when exposed to ambient light. The existing accounts concerning AgNP production by supramolecular peptide assemblies and hydrogels motivated us to test whether the individual Fmoc-Tyr and Fmoc-DOPA hydrogels and the combined hybrid hydrogel were able to reduce ionic silver to AgNP. To this end, we added silver nitrate solution to fully-formed hydrogels which were then incubated in the presence or absence of ambient light for five days (Fig. 6, Fig. S2). Following incubation, UV-Vis spectra revealed a significant absorption peak at approximately 467 nm for the light-exposed Fmoc-DOPA and a weaker lower peak at 453 nm for the hybrid gels, which was not present in the spectra of light-exposed Fmoc-Tyr hydrogel (Fig. 6a, Fig. S2). Moreover, these peaks were not present in the hydrogels unexposed to light or in respective control gels to which silver nitrate was not added (Fig. 6a, Fig. S2). Furthermore, corresponding appearance of a yellow-brown color was apparent for the light-exposed Fmoc-DOPA hydrogels and, to a lower extent, for the hybrid hydrogels, whereas no color change was observed for wells containing the other gels (Fig. 6b, Fig. S2). Similar absorption peaks have been reported for AgNP which were formed in the presence of various reducing agents,

including catechol-containing compounds.<sup>38, 59, 64</sup> Indeed, AgNP were detected in the Fmoc-DOPA and hybrid gel samples, as imaged by TEM, with the particles presenting distinct crystal-like morphology (Fig. 6c). Since AgNP did not form in case of the Fmoc-Tyr or the light-unexposed gels, their formation can be attributed to the functionality of the catechol moiety in the presence of light. Importantly, the hybrid gels presented similar functionality to that of the Fmoc-DOPA hydrogels, providing indication that this hybrid material is conferred with the redox capabilities observed for the hydrogels composed exclusively by Fmoc-DOPA.

To obtain a more detailed account of the redox-active hybrid gels, we monitored the kinetics of AgNP formation following the addition of silver nitrate to pre-formed gels (Fig. S3). We observed an increase in the absorbance at 445 nm, associated with the presence of AgNP in the gel. This signal increased over several hours and a plateau was reached approximately two days after the addition of silver nitrate (Fig. S3). This time period was longer than that observed for the Fmoc-DOPA individual gels, which reached a plateau after approximately one day (Fig. S3). In both cases, the overall kinetics of AgNP formation fitted the Boltzmann equation (Fig. S3, see Experimental section). Yet, in the first 8 hours, AgNP formation in the hybrid gel exhibited exponential behavior, while in the case of Fmoc-DOPA, a sigmoidal behavior was presented (Fig. S3 inset, see Experimental section). This may reflect a difference in the accessibility of the catechol functional groups in the two gel systems. Next, we compared the rheological properties of AgNP-containing and AgNP-absent hybrid gels. In this experiment, the hybrid gels were formed by diluting the combined stock solution into silver nitrate aqueous solutions or into water. To ensure the formation of AgNP, the gels were incubated for 2 days prior to measurement while exposed to ambient light. Frequency-sweep measurements at the linear regime (Fig. 6d, Fig. S4) revealed similar storage moduli for gels formed in the presence or

absence of silver nitrate, which were higher than their respective loss moduli by an order of magnitude (Fig. S4). This direct comparison of rheological properties shows that the high mechanical rigidity of the Fmoc-Tyr:Fmoc-DOPA hybrid gels is retained in their redox-active state, further demonstrating the functional synergy of the two gelators.

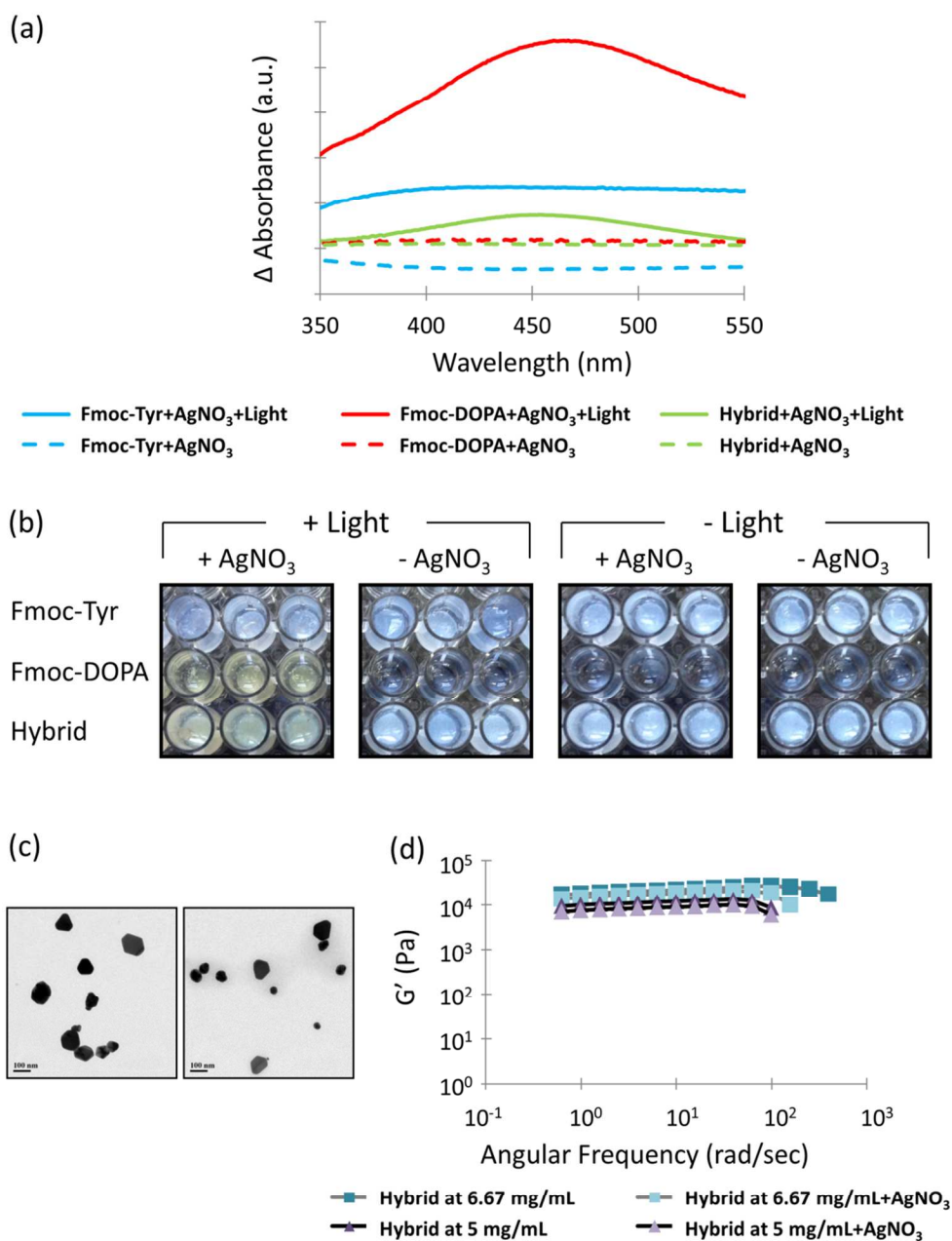


**Fig. 6** Ionic silver reduction by pre-prepared hydrogels. (a) UV-Vis spectra of hydrogels prepared from the individual Fmoc-Tyr and Fmoc-DOPA gelators (5 and 1.67 mg/mL respectively) and their 3:1 hybrid at 6.67 mg/mL after 5 days of incubation with 0.33 mM silver nitrate, in the presence or absence of light. The spectra are subtraction result of samples incubated without silver nitrate from the silver nitrate-added samples. (b) Photograph of a 96-well plate corresponding to the previous panel. (c) TEM micrographs of silver nanoparticles detected in samples of 1.67 mg/mL Fmoc-DOPA (left panel) and Fmoc-Tyr:Fmoc-DOPA 3:1 hybrid at 6.67 mg/mL (right panel) gels, following incubation with silver nitrate in the presence of light. Negative staining was not applied. (d) Frequency sweep characterization of Fmoc-Tyr:Fmoc-DOPA 3:1 hybrid gels at 5 or 6.7 mg/mL, formed in the presence or absence of 22 or 33 mM silver nitrate, respectively.

In summary, we demonstrated the ability to form Fmoc-Tyr:Fmoc-DOPA two-component hydrogels with mechanical properties that resemble those of Fmoc-Tyr gel, yet with functional properties of the catechol groups. This is a clear demonstration of the ability to utilize complementary properties of more than one building block to obtain novel functionalities. Beyond the reduction activity, such multicomponent organization should potentially allow to benefit from other functionalities of the Fmoc-DOPA building block including antioxidant activity, radical trapping and metal chelation. We believe that the combination of several building blocks to form complex non-covalent structures will be a central avenue in the field of peptide self-assembly in general and peptide hydrogel formation in particular.

## Conclusion

The ability to form multi-component hydrogels is an important step in the field of bio-inspired supramolecular assemblies. The molecular integration of building blocks with differential time-scale of organization and diverse characteristics allows to obtain functional assemblies of desired properties. The combination of the rapid Fmoc-Tyr hydrogelator and the functional Fmoc-DOPA component resulted in a progressive organization of the two components into functional

macroscopic structure with characteristics different from those of hydrogels formed by each of the modified amino acids separately.

### Acknowledgements

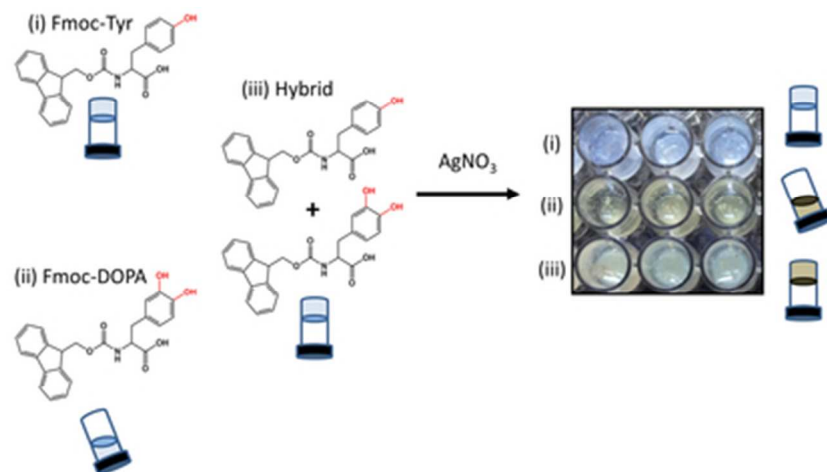
This work was supported in part by grants from the Israeli National Nanotechnology Initiative and Helmsley Charitable Trust for a Focal Technology Area on Nanomedicines for Personalized Theranostics (E.G) and the Marian Gertner Fellowship of the Marian Gertner Institute for Medical Nanosystems (G.F). We also thank members of the Gazit laboratory for helpful discussions.

### References

1. E. Gazit, *Chem. Soc. Rev.*, 2007, **36**, 1263-1269.
2. M. Zelzer and R. V. Ulijn, *Chem. Soc. Rev.*, 2010, **39**, 3351-3357.
3. P. W. J. M. Frederix, R. V. Ulijn, N. T. Hunt and T. Tuttle, *J. Phys. Chem. Lett.*, **2**, 2380-2384.
4. L. Adler-Abramovich and E. Gazit, *Chem. Soc. Rev.*, 2014, **43**, 6881-6893.
5. P. W. Frederix, G. G. Scott, Y. M. Abul-Haija, D. Kalafatovic, C. G. Pappas, N. Javid, N. T. Hunt, R. V. Ulijn and T. Tuttle, *Nat. Chem.*, 2015, **7**, 30-37.
6. J. P. Schneider, D. J. Pochan, B. Ozbas, K. Rajagopal, L. Pakstis and J. Kretsinger, *J. Am. Chem. Soc.*, 2002, **124**, 15030-15037.
7. H. Yokoi, T. Kinoshita and S. G. Zhang, *P. Natl. Acad. Sci. U.S.A.*, 2005, **102**, 8414-8419.
8. J. Kopecek and J. Y. Yang, *Acta Biomater.*, 2009, **5**, 805-816.
9. G. Fichman and E. Gazit, *Acta Biomater.*, 2014, **10**, 1671-1682.
10. J. Raeburn, G. Pont, L. Chen, Y. Cesbron, R. Levy and D. J. Adams, *Soft Matter*, 2012, **8**, 1168-1174.
11. J. Raeburn, A. Z. Cardoso and D. J. Adams, *Chem. Soc. Rev.*, 2013, **42**, 5143-5156.
12. J. Raeburn, C. Mendoza-Cuenca, B. N. Cattoz, M. A. Little, A. E. Terry, A. Z. Cardoso, P. C. Griffiths and D. J. Adams, *Soft Matter*, 2015, **11**, 927-935.
13. Z. Yang, H. Gu, D. Fu, P. Gao, J. K. Lam and B. Xu, *Adv. Mater.*, 2004, **16**, 1440-1444.
14. R. Vegners, I. Shestakova, I. Kalvinsh, R. M. Ezzell and P. A. Janmey, *J. Pept. Sci.*, 1995, **1**, 371-378.
15. L. Chen, G. Pont, K. Morris, G. Lotze, A. Squires, L. C. Serpell and D. J. Adams, *Chem. Commun.*, 2011, **47**, 12071-12073.

16. V. Jayawarna, M. Ali, T. A. Jowitt, A. F. Miller, A. Saiani, J. E. Gough and R. V. Ulijn, *Adv. Mater.*, 2006, **18**, 611-614.
17. D. J. Adams, M. F. Butler, W. J. Frith, M. Kirkland, L. Mullen and P. Sanderson, *Soft Matter*, 2009, **5**, 1856-1862.
18. A. Mahler, M. Reches, M. Rechter, S. Cohen and E. Gazit, *Adv. Mater.*, 2006, **18**, 1365-1370.
19. Y. Qiu and K. Park, *Adv. Drug Deliv. Rev.*, 2012, **64**, 49-60.
20. J. L. Drury and D. J. Mooney, *Biomaterials*, 2003, **24**, 4337-4351.
21. D. J. Adams, *Macromol. Biosci.*, 2011, **11**, 160-173.
22. V. Jayawarna, S. M. Richardson, A. R. Hirst, N. W. Hodson, A. Saiani, J. E. Gough and R. V. Ulijn, *Acta Biomater.*, 2009, **5**, 934-943.
23. T. Liebmann, S. Rydholm, V. Akpe and H. Brismar, *Bmc Biotechnol.*, 2007, **7**, 88.
24. R. M. Burch, M. Weitzberg, N. Blok, R. Muhlhauser, D. Martin, S. G. Farmer, J. M. Bator, J. R. Connor, M. Green, C. Ko and et al., *Proc. Natl. Acad. Sci. U. S. A.*, 1991, **88**, 355-359.
25. C. T. Yen, T. L. Hwang, Y. C. Wu and P. W. Hsieh, *Eur. J. Med. Chem.*, 2009, **44**, 1933-1940.
26. S. Fleming and R. V. Ulijn, *Chem. Soc. Rev.*, 2014, **43**, 8150-8177.
27. S. Sutton, N. L. Campbell, A. I. Cooper, M. Kirkland, W. J. Frith and D. J. Adams, *Langmuir*, 2009, **25**, 10285-10291.
28. K. Thornton, A. Smith, C. R. Merry and R. Ulijn, *Biochem. Soc. Trans.*, 2009, **37**, 660-664.
29. A. Aufderhorst-Roberts, W. J. Frith and A. M. Donald, *Soft Matter*, 2012, **8**, 5940-5946.
30. D. M. Ryan, S. B. Anderson, F. T. Senguen, R. E. Youngman and B. L. Nilsson, *Soft Matter*, 2010, **6**, 475-479.
31. R. Orbach, L. Adler-Abramovich, S. Zigerson, I. Mironi-Harpaz, D. Seliktar and E. Gazit, *Biomacromolecules*, 2009, **10**, 2646-2651.
32. A. Saha, S. Bolisetty, S. Handschin and R. Mezzenga, *Soft Matter*, 2013, **9**, 10239-10242.
33. G. Fichman, T. Guterman, J. Damron, L. Adler-Abramovich, J. Schmidt, E. Kesselman, L.J.W. Shimon, A. Ramamoorthy, Y. Talmon and E. Gazit., 2015, *Submitted*.
34. E. Faure, C. Falentin-Daudré, C. Jérôme, J. Lyskawa, D. Fournier, P. Woisel and C. Detrembleur, *Prog. Polym. Sci.*, 2013, **38**, 236-270.
35. J. Sedó, J. Saiz-Poseu, F. Busqué and D. Ruiz-Molina, *Adv. Mater.*, 2013, **25**, 653-701.
36. H. Ceylan, M. Urel, T. S. Erkal, A. B. Tekinay, A. Dana and M. O. Guler, *Adv. Funct. Mater.*, 2013, **23**, 2081-2090.
37. G. Fichman, T. Guterman, L. Adler-Abramovich and E. Gazit, *Nanomaterials*, 2014, **4**, 726-740.
38. G. Fichman, L. Adler-Abramovich, S. Manohar, I. Mironi-Harpaz, T. Guterman, D. Seliktar, P. B. Messersmith and E. Gazit, *ACS Nano*, 2014, **8**, 7220-7228.
39. J. Raeburn and D. J. Adams, *Chem. Commun.*, 2014, **51**, 5170-5180.
40. D. G. Velázquez and R. Luque, *Chem. Eur. J.*, 2011, **17**, 3847-3849.
41. D. Li, Y. Shi and L. Wang, *Chin. J. Chem.*, 2014, **32**, 123-127.
42. C. Colquhoun, E. R. Draper, E. G. Eden, B. N. Cattoz, K. L. Morris, L. Chen, T. O. McDonald, A. E. Terry, P. C. Griffiths and L. C. Serpell, *Nanoscale*, 2014, **6**, 13719-13725.
43. S. Boothroyd, A. Saiani and A. F. Miller, *Biopolymers*, 2014, **101**, 669-680.

44. Z. Džolić, K. Wolsperger and M. Žinić, *New J. Chem.*, 2006, **30**, 1411-1419.
45. M. Zhou, A. M. Smith, A. K. Das, N. W. Hodson, R. F. Collins, R. V. Ulijn and J. E. Gough, *Biomaterials*, 2009, **30**, 2523-2530.
46. R. K. Das, R. Kandanelli, J. Linnanto, K. Bose and U. Maitra, *Langmuir*, 2010, **26**, 16141-16149.
47. B. Adhikari, J. Nanda and A. Banerjee, *Soft Matter*, 2011, **7**, 8913-8922.
48. Y. M. Abul-Haija, S. Roy, P. W. Frederix, N. Javid, V. Jayawarna and R. V. Ulijn, *Small*, 2014, **10**, 973-979.
49. D. M. Ryan, T. M. Doran and B. L. Nilsson, *Chem. Commun.* 2011, **47**, 475-477.
50. D. M. Ryan, T. M. Doran and B. L. Nilsson, *Langmuir*, 2011, **27**, 11145-11156.
51. L. Chen, J. Raeburn, S. Sutton, D. G. Spiller, J. Williams, J. S. Sharp, P. C. Griffiths, R. K. Heenan, S. M. King, A. Paul, S. Fuzeland, D. Atkins and D. J. Adams, *Soft Matter*, 2011, **7**, 9721-9727.
52. G. Socrates, *Infrared and Raman characteristic group frequencies: tables and charts*, John Wiley & Sons, 2004.
53. J. Kong and S. Yu, *Acta Biochim. Biophys.*, 2007, **39**, 549-559.
54. S. Fleming, P. W. J. M. Frederix, I. Ramos Sasselli, N. T. Hunt, R. V. Ulijn and T. Tuttle, *Langmuir*, 2013, **29**, 9510-9515.
55. S. M. M. Reddy, G. Shanmugam and A. B. Mandal, *Soft Matter*, 2015, **11**, 4154-4157.
56. S. Eckhardt, P. S. Brunetto, J. Gagnon, M. Priebe, B. Giese and K. M. Fromm, *Chem. Rev.*, 2013, **113**, 4708-4754.
57. Q. H. Tran, V. Q. Nguyen and A.-T. Le, *Adv. Nat. Sci: Nanosci. Nanotechnol.*, 2013, **4**.
58. H. Basit, A. Pal, S. Sen and S. Bhattacharya, *Chem. Eur. J.*, 2008, **14**, 6534-6545.
59. K. C. Black, Z. Liu and P. B. Messersmith, *Chem. Mater.*, 2011, **23**, 1130-1135.
60. D. E. Fullenkamp, J. G. Rivera, Y.-k. Gong, K. A. Lau, L. He, R. Varshney and P. B. Messersmith, *Biomaterials*, 2012, **33**, 3783-3791.
61. B. Adhikari and A. Banerjee, *Chem. Eur. J.*, 2010, **16**, 13698-13705.
62. S. Roy and A. Banerjee, *Soft Matter*, 2011, **7**, 5300-5308.
63. A. Biswas and A. Banerjee, *Soft Matter*, 2015, **11**, 4226-4234.
64. H. Bar, D. K. Bhui, G. P. Sahoo, P. Sarkar, S. P. De and A. Misra, *Colloids Surf., A.*, 2009, **339**, 134-139.



Hybrid hydrogels composed of the Fmoc-Tyr and Fmoc-DOPA building blocks present mechanical rigidity and redox activity

39x19mm (300 x 300 DPI)